

## **Controls on greigite preservation in a gas-hydrate system off Krishna-Godavari basin, Bay of Bengal**

**Firoz Badesab<sup>1\*</sup>, Virsen Gaikwad<sup>1</sup>, Pawan Dewangan<sup>1</sup>**

<sup>1</sup> CSIR - National Institute of Oceanography, Dona Paula 403004, Goa, India

\*Corresponding author: Firoz Badesab (firoz@nio.org)

### **Abstract**

Shallow sediments across large parts of Krishna-Godavari (K-G) Basin offshore east central Indian contains abundant methane and gas hydrates. In this study, we carried out rock-magnetic and transmission electron microscope (TEM) analyses on the samples from a sediment core (MD161/Stn-8) to constrain the formation and preservation of greigite in shallow sediments and how this might link to reactions involving methane. Here, we report for the first time the occurrence of silicate-hosted iron sulfides (greigite) inclusions which is an important observation for understanding the preservation of magnetic minerals in gas hydrate systems. The magnetization of the greigite zone (17 – 23 mbsf) is carried by complex magnetic mineral assemblages of detrital iron oxides (titanomagnetite), diagenetic iron sulfide (greigite) occurring as nano-inclusions within larger silicate particles and biogenic minerals. Elevated concentrations of dissolved pore water silica and alkalinity within the magnetically enhanced greigite zone suggests that silica diagenesis and silicate weathering triggered by paleo-methane seepage played a key role in crystallizing the diagenetically formed iron sulfide (greigite) into silicate matrix. The silicate-hosted magnetic inclusions protected the ferrimagnetic greigite from further diagenetic dissolution and prevented its conversion into stable pyrite. Three scenarios explaining the potential controls on the greigite preservation in gas hydrate marine sedimentary system has been proposed.

### **Key Points:**

- For the first time, we report the occurrence of silicate-hosted greigite inclusion and highlights its importance in understanding magnetic mineral diagenesis in gas hydrate systems.
- We propose that coupled silicate weathering and silica diagenesis triggered by AOM played an important role in preservation of greigite occurring as inclusions in silicate minerals in a gas hydrate system off Krishna-Godavari basin, Bay of Bengal.
- The present study unravels the complex magnetic mineral assemblages (detrital, diagenetic, biogenic) in a marine gas hydrate sedimentary system.
- We present rock-magnetic and geochemical signatures of diagenetic control of greigite production and preservation in a gas hydrate system off Krishna-Godavari basin, Bay of Bengal.
- Three scenarios explaining the potential controls on the greigite preservation in gas hydrate marine sedimentary system are proposed.

## 1. Introduction

Greigite ( $\text{Fe}_3\text{S}_4$ ) is a ferrimagnetic iron sulfide mineral that forms in sulfate reducing environments as a precursor to pyrite ( $\text{FeS}_2$ ) (Berner, 1984). Geochemical conditions favourable for the formation and preservation of greigite are a limited source of sulphide, whether it derives from microbially-mediated processes such as sulphate reduction, anaerobic oxidation of methane (AOM), and formation of gas hydrates (Kasten et al. 1998; Jørgensen et al. 2004; Horng and Chen 2006; Larrasoña et al. 2006; Housen and Musgrave 1996). Widespread occurrence of greigite has been reported in gas hydrate bearing sediments in Cascadia Margin, Nankai Trough, offshore Japan, and offshore southwestern, Taiwan (Housen and Musgrave 1996; Musgrave et al. 2006; Larrasoña et al. 2006; Horng and Chen 2006; Kars and Kodama 2015). The occurrence of greigite is useful for detecting paleo-gas hydrate zones within the gas hydrate stability zone (Housen and Musgrave, 1996; Musgrave et al. 2006; Larrasoña et al. 2006; Kars and Kodama, 2015). Rockmagnetic study by Housen and Musgrave (1996) in Cascadia Margin demonstrated that the hydrogen sulfide which is required to complete the pyritization process sometimes gets trapped and remains preserved within the hydrate itself. Hydrate formation provides cementation to the trapped hydrogen sulfide and inhibits its exposure with the surrounding pore-fluids (host sediment) thereby favouring the growth and preservation of iron sulfides (greigite, pyrrhotite). Larrasoana et al. (2007) suggested that formation of methane hydrates limits the availability of hydrogen sulfide and cause arrestation of pyritization processes and favours greigite. In Nankai Trough, offshore Japan, Kars and Kodama (2015) reported that authigenic ferri-magnetic iron sulfides (greigite and pyrrhotite) formed during late diagenesis sometimes remains trapped in gas-hydrates. As hydrates dissociates, due to changing P-T conditions, the iron sulfide (greigite) gets exposed and is no longer stable, and subsequently get transformed into stable pyrite. New gas hydrate zones are created when the conditions become favourable again for the formation of gas hydrates (Housen and Musgrave, 1996; Musgrave et al. 2006; Larrasoña et al. 2006; Kars and Kodama, 2015).

Drilling and sediment coring activities onboard D/V JOIDES Resolution during India National Gas Hydrate Expedition 01 confirmed the presence of fracture-filled gas hydrates in K-G basin (Collett et al. 2008; Kumar et al. 2014). Recently Badesab et al. 2017; 2019 conducted rock-magnetic and sedimentological investigation on sediment core NGHP-01-10D (vicinity of site MD161/Stn-8 (present study) and examined the magnetic signals of detrital and diagenetic processes associated with the development of a fracture-filled gas hydrate system of K-G basin. A detailed rockmagnetic and sedimentological investigation was conducted by Dewangan et al. (2013) on sediment core

(MD161/Stn-8) from proven gas hydrate region to examine the magnetic minerals diagenesis in a gas hydrate environment of K-G basin. The site MD161/Stn-8 was basically a re-coring of the upper sediments recovered from site NGHP-01-10D. A magnetically enhanced zone between 17.68 mbsf and 23.6 mbsf at site MD161/Stn-8 dominated by fine-grained superparamagnetic (SP) sized ferrimagnetic greigite within the pyritization (low magnetization) zone was identified (Dewangan et al. 2013). Their work reported that short-term fluctuations in sulfate-methane transition zone (SMTZ) controlled by variability in methane fluxes caused limited production of hydrogen sulfide which favoured greigite formation in K-G basin (Dewangan et al. 2013). However, studies on the properties and conditions favouring the preservation of greigite in gas hydrate bearing sedimentary system are very limited.

The sediment core (MD161/Stn-8) overlying the methane hydrate deposits in K-G preserves a magnetic signatures of detrital, diagenetic, and biogenic minerals which influenced the sediment magnetic record. In this study, we carried out detailed first order reversal curves (FORC) analysis and transmission electron microscope (TEM) observations on a greigite bearing sediment interval of core (MD161/Stn-8) and integrated with geochemical records to unravel the mechanism of greigite preservation in a gas hydrate system of K-G basin. An attempt has also been made to investigate how this might link to reactions involving methane.

## **2. Study area and core location**

The Krishna-Godavari basin (K-G) basin, located along the central east coast of India occupies an onshore area of about 28,000 km<sup>2</sup> and extends offshore covering an area of 1,45,000 km<sup>2</sup> (Rao 2001). The Krishna and Godavari rivers supply bulk of detrital sediment load to the K-G basin. Sediment thickness in the K-G basin varies from 3 to 5 km in the onshore region to as much as 8 km in the offshore region (Prabhakar and Zutshi 1993). The annual sediment transport of the Krishna and Godavari rivers is calculated to be 67.7 and 170 × 10<sup>6</sup> metric tonnes, respectively (Biksham & Subramanian 1988; Ramesh & Subramanian 1988). A 30 m sediment core (MD161/Stn-8) overlying the methane hydrate deposits was retrieved onboard R/V Marion Dufresne from the K-G basin (Fig.1). The location of the sediment core (MD161/Stn-8) lies in the vicinity of site NGHP-01-10, where ~128 m thick sub-surface gas hydrates were identified (Lee and Collett 2009). In this study, we utilized the pore-water dissolved silica concentration data of site NGHP-01-10D (Lat: 15°51.8609N, Long: 81°50.0749E), which is close (less than 105.2 m apart) to site MD161/Stn-8 (Lat: 15°51.8624N, Long: 81°50.0692E). A good correlation of magnetic susceptibility between these two sediment cores is also noticed (See Supplementary Fig.S2). Hence, it is realistic to believe

that pore-water dissolved silica ( $\text{H}_4\text{SiO}_4$ ) concentration between the two sites (MD161/Stn-8 and NGHP-01-10D) will not vary much and was therefore used in the present study.

## 2.1 Methods

The sediment core was sub-sampled using 1-inch cylindrical plastic sample bottles and magnetic measurements were made at Indian Institute of Geomagnetism, Panvel, India. More details on the rock-magnetic and pore-water geochemical analyses can be found at Peketi et al. 2012; Dewangan et al. 2013; Solomon et al. 2014. The sediment lithology is composed of nannofossil-bearing-to-rich clay that ranges in color from very dark gray to black (Collet et al. 2008). Silt and clay size fractions constitute bulk of the sediments. Silt and clay content in sediment core (MD161/Stn-8) varies between 24-54 vol% and 45-73 vol% respectively (Joshi et al. 2014). Numerous layers of authigenic carbonates varying in size from few mm's to over 5 cm are noticed with fossil assemblages. Between 15 - 20 mbsf, several hard authigenic carbonates of varying morphologies are identified (Mazumdar et al. 2009). A sharp drop in porosity (25–50%) within this sediment interval compared to the relative background porosity of about 75% is noticed. Several well-preserved shells of chemosynthetic clam *Callyptogena* sp. indicative of a paleo-cold seep event were found in this zone (Mazumdar et al. 2009).

First order reversal curves (FORC) measurements were carried out on the selected bulk sediment samples from greigite bearing zone (17-23 mbsf) with a Princeton Measurements Corporation Alternating Gradient Force Magnetometer (Model MicroMag 2900, sensitivity  $1 \times 10^{-11} \text{Am}^2$ ) at Institute for Rock Magnetism, USA. FORC diagrams were obtained with a 1 T saturating field (~300 - 500 FORCs, field increments of 0.5 mT, averaging time of 250 ms). FORC diagrams were calculated using the FORCinel software (smoothing factor SF=3, (Harrison and Feinberg, 2008; Roberts et al. 2000; Chang et al. 2016a).

Following the extraction method of Petersen et al. (1986), magnetic particles were separated from the bulk sediments from greigite bearing interval (17- 23 mbsf). A scanning electron microscope (SEM) JEOL JSM-5800 LV was used to capture the images of the magnetic particles in secondary electron (SE) imaging mode at energy levels between 15 and 20 kV. Transmission electron Microscope (TEM) observations were carried out on a magnetic separates with a JEOL JEM-2100F TEM with a field emission gun (operating voltage 200 kV) at Indian Institute of Science, Bangalore, India. An Oxford INCA Energy TEM250 microanalysis system. EDS and Gatan CCD camera was used.

### **3. Results**

#### **3.1. FORC Diagrams**

FORC measurements were made on the magnetic extracts to characterize the constituent magnetic mineral assemblages. FORC diagrams for the representative samples from greigite bearing zone of core MD161/Stn-8 are shown in Figs. 2f,g and 3a-3c. The FORC diagram (Fig. 2f) shows a broad distribution with concentric contours between 15–80 mT and a peak HC at about 40 mT. The large vertical spread is indicative of strong magnetostatic interactions (Pike et al. 1999; Roberts et al. 2000). It is interesting to note that the centre of the distribution appears to be shifted downward towards negative  $H_u$  values (Fig. 2f) indicating strongly interacting SD magnetic mineral assemblages (Pike et al. 1999; Roberts et al. 2000). FORC diagram for the sample (Fig. 2g) showed a dominant narrow central ridge along  $H_u$  axis with poor vertical spreading and elongated contour along  $H_c$  axis. Such FORC signature reflects non-interacting or weakly interacting SD particles (Pike et al. 1999; Egli et al. 2010; Chang et al. 2014a). FORC distributions for samples from 20.98 mbsf and 22.38 mbsf are characterized by a peak at  $B_C \sim 10$  mT with closed contours indicating vortex-state behavior of magnetic particles behaviour (Lascu et al. 2018; Muxworthy and Dunlop, 2002; Roberts et al. 2000; Roberts et al. 2017) (Figs. 3a, 3b). The FORC diagram for sample from 22.44 mbsf (Fig. 3c) showed a central ridge signature with a peak fields changing between  $\sim 10$  and 40 mT suggesting the presence of biogenic magnetite (Chang et al. 2014b).

#### **3.2. Scanning electron microscopy (SEM) analyses of magnetic separates from greigite zone**

SEM analyses on magnetic particles extracted from greigite bearing sediment interval indicates the presence of complex magnetic mineralogies. The magnetic mineralogy is dominated by detrital ferrimagnetic iron oxides (Figs. 4a, 4d) and diagenetic magnetic iron sulfides (pyrite) (Figs. 4b,c,e,f) of various sizes and greigite occurring within interstices of pyrite crystals (Dewangan et al. 2013). Pyrite crystals formed as a result of diagenesis occur as individual grains as well as in the form of aggregates (Figs. 4b, 4c, 4e, 4f). We observed several grains probably of magnetite or greigite core (Ebert et al. 2018; Roberts and Turner, 1993) with pyrite overgrowths (Fig. 5) in this zone.

#### **3.3. Transmission electron microscopy (TEM) analyses of magnetic particles from greigite zone.**

TEM observations were performed on the magnetic particles extracted from greigite zone. Abundant nanoparticles of magnetic iron oxides and iron sulfides are observed (Figs. 6a-6f). Fine-grained preferably superparamagnetic (SP) size iron sulfides (pyrite, greigite) occurring as inclusions within

the matrix of host siliceous grain were observed (Figs. 6a, 6b). The majority of the magnetic (oxide, sulfide) inclusions appears to be distributed randomly within high susceptibility zone (Fig. 6a,6b and Fig. 2a). TEM-EDS analysis indicates the presence of Si, Ti, Ca, Fe, S, Al in all the analyzed samples (Figs. 6a-6f, Spectra 1-6). The sample from 22.52 mbsf showed cluster of irregularly shaped, poorly crystallized Fe-S grains with no defined morphology (Fig. 6c). This probably might have been formed by magnetotactic bacteria (MTB) as a result of extracellular biologically induced mineralization (BIM) and indicates biogenic origin (Bazylinski et al. 1995; Muxworthy et al. 2013). Irregularly shaped greigite crystals occurring as aggregate is noticed (Fig. 6d). Sub-rounded biogenic iron sulfide and magnetite nanoparticles with size range of ~100-140 nm are noticed (Bazylinski et al. 1995) (Figs. 6e, 6f).

## **4. Discussion**

### **4.1. Detrital input, silica diagenesis, silicate weathering, formation and preservation of iron sulfides (greigite) at site MD161/Stn-8.**

Our rock-magnetic, FORC, TEM-EDS and SEM observations confirmed the presence of complex magnetic mineralogy of detrital, diagenetic and biogenic origin in the studied samples. The detrital Fe-Ti rich magnetic minerals in the studied sediment interval of core MD/161/Stn-8 are mainly sourced from Deccan basalts and were supplied by the Krishna and Godavari rivers system (Figs. 4a,d) (Dewangan et al. 2013; Badesab et al. 2017; Badesab et al. 2019). Magnetic iron mineral inclusions that are hosted in the silicate minerals occur widely in igneous and metamorphic rocks and have been studied extensively (Evans and Wayman, 1970; Morgan and Smith, 1981; Chang et al. 2016). However, studies focussing on the properties and conditions favouring the preservation of iron sulfides (greigite) in gas hydrate bearing sedimentary system are very limited. In silicate hosted magnetic mineral inclusions, silicate matrix protect the magnetic inclusions against the changes in surrounding geochemical environments and are therefore used as potential markers for tracking the sediment sources (Hounslow and Morton, 2004; Chang et al. 2016). One key assumption that is often considered is that silicate hosted magnetic-mineral inclusions found in marine sediments carries a source specific signature mainly terrestrial (igneous and metamorphic rocks) sources. For the first time, we report the occurrence of diagenetically formed iron sulfides (greigite) nanoparticles as inclusions within silicate minerals in greigite bearing sediment interval of core MD161/Stn-8 (Figs. 6a,b). Detailed magnetic discrimination of diagenetic and biogenic minerals at site MD161/Stn-8 is discussed in section 4.2.

Silica diagenesis at methane seep sites plays an important role in the formation of magnetic mineral inclusions. A study by Smryzka et al. (2015) in methane-seep limestones, USA demonstrated that dissolved silica concentrations is generally three times higher at the AOM hot spots (methane seepage sites) than the background marine sediments. Intense AOM activity at methane seepage sites significantly increases the pH of pore waters and subsequently leads to dissolution of biogenic silica, followed by the re-precipitation of the dissolved silica in the proximity of the AOM hotspot. They concluded that higher methane fluxes are required for a significant increase in pH of the pore waters which allows degassing of carbon dioxide produced from carbonate precipitation.

At site MD161/Stn-8, SMTZ is ~ 15-16 mbsf which is indicative of depth of the present-day AOM (Mazumdar et al. 2009). The greigite bearing sediment interval, i.e., 17-23 mbsf was formed around 46.2 - 53 kyr ago when the AOM was very intense and active methane seepage was occurring (Mazumdar et al., 2009). Occurrence of chemosynthetic community, seep-related authigenic carbonates, molybdenum (Mo) anomaly and enrichment of  $\delta^{34}\text{S}_{\text{CRS}}$  support paleo-methane seepage event in this zone (Mazumdar et al. 2009; Peketi et al. 2012). The paleo-cold seep created conducive environment for silica diagenesis and silicate weathering to occur concurrently. These might have led to the dissolution and re-precipitation of dissolved silica which embedded the diagenetically formed iron sulfides (greigite) as inclusions within silicate matrix. Similar processes of AOM-influenced silica diagenesis and silicate weathering have been reported in the Sea of Okhotsk and Black Sea (Aloisi et al. 2004; Wallmann et al. 2008), Cretaceous methane-seep deposits from New Zealand (Kiel et al. 2013), methane-rich sediments from southeast Bering Sea (Cook et al. 2011), and methane-seep limestones, USA (Smryzka et al. 2015; Kuechler et al. 2012). Elevated concentrations of dissolved pore water silica and alkalinity in the vicinity of present-day AOM suggests that silica diagenesis and silicate weathering triggered by AOM processes which plays a critical role in the inclusion of magnetic mineral within silicates (Figs. 6a,b and Fig. 7). In the present study, we demonstrated that the diagenetically formed greigite can occur as inclusions within silicate minerals and survive in hostile gas hydrate systems.

In anoxic marine sedimentary systems, silicate weathering is well-documented in marine sediments for example offshore India, Ulleung Basin, Chile, Cascadia, Sea of Okhotsk and Black Sea (Solomon et al. 2014; Kim et al. 2016; Scholz et al. 2013, Wallmann et al. 2008; Aloisi et al. 2004). A comprehensive pore-water geochemical study by Solomon et al. (2014) reported that  $\text{CO}_2$  produced during net microbial methanogenesis at site NGHP-01-10D (proximal to present study site MD161/Stn-8) is neutralized through weathering of detrital silicate minerals leading to decrease in

pore-water pH and enhancement in production of alkalinity leading to dissolution of silicate minerals and authigenic carbonate formation in methanogenic sediments of K-G basin. Similar observations were made by Aloisi et al. (2004) in Black Sea sediments. In Sea of Okhotsk, Wallmann et al. (2008) reported that weathering of plagioclase, feldspar, pyroxene, quartz and olivine may also lead to precipitation of authigenic clays. An observed increase in pore-water alkalinity, Si (Figs. 7a,b,c) and dissolved inorganic carbon (DIC) (Solomon et al. 2014) in the vicinity of present-day AOM reflects weathering of silicate minerals in these interval (Wallmann et al. 2018; Scholz et al. 2013). In past, coupled silicate weathering and silica diagenesis due to intense AOM might have played an important role in preservation of greigite occurring as inclusions within silicate minerals as indicated by the presence of quartz in the TEM-EDS data. If greigite is occurring as coating on the surface of silicate minerals, then we would expect oxidation of greigite due to long-term (2007 - 2009) storage of samples. In such a scenario, we would have observed much larger decrease in magnetic susceptibility of bulk sediments. A minor decrease in susceptibility (Dewangan et al. 2013) suggests that greigite is primarily occurring as inclusions rather than on the surface of silicate minerals.

The growth of paramagnetic pyrite rim over ferrimagnetic greigite and magnetite core in rapidly depositing sediments has been reported from South Island, New Zealand (Roberts and Turner, 1993) and the Dead Sea basin (Eberts et al. 2018). The magnetic grains extracted from greigite zone of core MD161/Stn-8 showed pyrite (orange-reddish color) overgrowths probably on magnetite / greigite core (Fig. 5). This finding is similar to the observations made by Larrasoana et al. (2007) which demonstrated that the dissolved sulfide prefers to react more easily with highly reactive iron which is readily available on the surface of iron-bearing core.

#### **4.2. Discrimination between diagenetic versus biogenic magnetic minerals**

In marine sedimentary systems, production and preservation of diagenetic greigite is quite complex (Chang et al. 2014a). As a precursor to pyrite, metastable greigite ( $\text{Fe}_3\text{S}_4$ ) is formed during the pyritization process (Berner, 1984). Greigite could remain preserved in sediments if suitable conditions like low pore-water sulfide concentrations and enhanced availability of iron persists (Kao et al. 2004; Rowan and Roberts, 2006). A detailed rock-magnetic study by Dewangan et al. (2013) on sediment core MD 161/Stn-8 from paleo-cold seep site from K-G basin (present study) demonstrated that variability of methane flux caused sudden shifting of SMTZ thereby, inhibiting the accumulation of excess sulfide which leads to greigite formation. In the magnetically enhanced greigite zone, Dewangan et al. (2013) observed a minor drop in the lab-based mass-magnetic susceptibility (Nov, 2009) as compared to the volume-magnetic susceptibility measured onboard



(May,2007) reflecting the loss of magnetic minerals during sample storage. Such a reduction in magnetic susceptibility is another indication for the oxidation of greigite during storage.

In this section, we focus on interpreting the FORC and TEM observations to constrain the formative mechanism (diagenetic, biogenic) of magnetic minerals identified within the greigite bearing sediment interval at site MD161/Stn-8. A strong magnetostatic interaction in a diagenetically formed greigite exhibits FORC with large vertical spreading (Roberts et al. 2000, 2006; Rowan and Roberts, 2006; Chang et al. 2007; Vasiliev et al. 2007). In our sample, the FORC diagram (Fig. 2f) shows a broad distribution with concentric contours between 15–80 mT and a peak HC at about 40 mT suggesting the presence of greigite of diagenetic origin. It is interesting to note that the centre of the distribution appears to be shifted downward towards negative  $H_u$  values (Fig. 2f) indicating strongly interacting SD magnetic mineral assemblages (Pike et al. 1999; Roberts et al., 2000). Similar FORC signatures were observed in the sediment samples from the Messinian Black sea which contained diagenetic greigite (Chang et al. 2014a) and supports our interpretation of diagenetically formed greigite mineral.

In addition, magnetotactic bacteria (MTB's) can also precipitate greigite ( $Fe_3S_4$ ) and magnetite ( $Fe_3O_4$ ) in their magnetosomes; however, limited information is available on their formation and preservation in marine sedimentary system (Rowan and Roberts, 2006; Roberts, 2011a; Reinholdsson et al. 2013). High values of rock-magnetic parameter  $SIRM/\chi$  in a magnetically enhanced zone is diagnostic of biogenic (magnetite, greigite) minerals (Snowball, 1997a) and are characterized by a stable SD grain size (Maher, 1988; Oldfield, 2007). At site MD161/Stn-8, high values of  $SIRM/\chi$  within 22-23 mbsf can be attributed to the presence of SD size magnetic particles of biogenic origin (Snowball, 1997a), while enhancement of  $\chi_{fd}\%$  within 17 - 21 mbsf (Dewangan et al. 2013) reflects the dominance of SP size ferrimagnetic minerals. Preservation of fine-grained iron sulfides particles in this zone suggest that greigite occurs as inclusions in silicate mineral or with silica coating.

In the studied samples, TEM-EDS spectra (Figs. 6b-d ) of the mineral particles from magnetically enhanced zone showed that the presence of two main elements i.e., Fe and S, indicating the presence of iron sulfides. The biogenic greigite crystals possess less regular morphologies in comparison with distinct and well-developed crystal morphologies of bacterial magnetite (Petersen et al. 1986; Stoltz et al. 1986; Roberts et al. 2011b; Chang et al. 2012; Larrasoana et al. 2012; Yamazaki, 2012). Cluster of irregularly shapes, poorly crystallized iron sulfide grains (Figs. 6c,d) appears to be mediated by microbial action and the precipitation mechanism is more likely of extracellular mineralization

induced by magnetotactic bacteria (Bazylinski et al. 1995; Vasiliev et al. 2008; Reinholdsson et al. 2013; Muxworthy et al. 2013). TEM observations were made on magnetic extracts, while FORC measurements were carried on the bulk sediment samples which showed the presence of both diagenetic and biogenic greigite (Fig. 2f,g). The identification of biogenic greigite is supported by TEM observations which indicate the presence of greigite nanocrystals whose size and morphology are consistent with a biogenic origin (Figs. 6c-e).

The FORC diagram for sample from 22.44 mbsf showed a central ridge signature with a peak fields changing between  $\sim 10$  mT and 40 mT indicating the presence of biogenic magnetite (Fig. 3c) (Chang et al. 2014b). The TEM observations further confirm the presence of biogenic magnetite crystals in this sample (Fig. 6f). In sapropels-rich sediments of the Baltic Sea, Reinholdsson et al. (2013) demonstrated that both biogenic greigite and magnetite containing sediments exhibit similar FORC signature. In the present study, Fe and S bearing samples (22.34 mbsf, 22.52mbsf and 22.70 mbsf) show a similar FORC signature with a central ridge further confirming that the magnetic mineral is biogenic greigite (Figs. 6c-e). Some samples with Fe and O (Fig. 6f) also suggest the existence of biogenic magnetite.

#### **4.3 Linkage between magnetic enhancement, organic matter supply and preservation of magnetic iron oxides and sulfides at site MD161/Stn-8.**

Several studies reported the linkage between magnetic enhancements and production of ferrimagnetic mineral and organic matter supply. The rock-magnetic data of sediment cores from eastern Mediterranean Sea observed a strong linkage between magnetic enhancement caused by formation of authigenic (SD, ferrimagnetic) magnetic iron sulfides and organic carbon content (Roberts et al. 1999). Similarly, in Swedish lake sediments, a positive relationship between total organic carbon and precipitation of fine-grained SD ferrimagnetic magnetite of bacterial origin has been reported (Snowball, 1994; Snowball et al. 1999; Snowball et al. 2002). More recently, Reinholdsson et al. 2013 noticed a similar relationship in the Baltic Sea sediments and emphasized a linkage between primary production, organic matter preservation and production of ferrimagnetic minerals at sites in North Central Baltic Proper (NCBP) and Faro Deep (FD), eastern Gotland Basin. Next, we investigated whether such linkages exist between the magnetic enhancement and preservation of organic carbon at site MD161/Stn-8. A noticeable drop in TOC content (See supplementary Fig. S1) in the magnetically strong zone (17-23 mbsf) suggests that the occurrence of fine-grained SD magnetite and iron sulfides (greigite) in this interval is controlled by both biogenic and non-steady state diagenetic process.

#### **4.4. A conceptual model explaining constraints on greigite preservation in gas hydrate system of K-G basin.**

Three scenarios explaining the potential controls on the greigite preservation in gas hydrate marine sedimentary system has been proposed (Fig. 8). In K-G basin, shale-tectonics created fracture and faults which provided conduits for upward migration of methane-enriched fluids from deeper sources (Dewangan et al. 2011; Sriram et al. 2013; Mazumdar et al. 2019). High methane flux led to intensification of AOM via sulfate reduction in the vicinity of the seafloor generating elevated H<sub>2</sub>S concentration. At site MD161/Stn-8, SMTZ is ~ 15-16 mbsf is indicative of depth of present-day AOM. In past around 46.2 – 53.0 kyr, a intense AOM was occurring close to the sea floor as evident from multiple signatures of methane seeps. The greigite bearing sediment interval is observed within this zone between 17 and 23 mbsf. The presence of chemosynthetic communities and archaeal mat in the vicinity of greigite zone at sites MD161/Stn-8 and NGHP-01-10D is associated with the occurrences of H<sub>2</sub>S seepages (Collett et al. 2008; Peketi et al. 2012; Mazumdar et al. 2009:2011). At present site (MD161/Stn-8), Peketi et al. (2012) observed molybdenum anomaly, a diagnostic feature of hydrogen sulfide seepage, suggesting at least two distinct events of H<sub>2</sub>S build up at the sediment-water interface. Abrupt shift of SMTZ might have limited the production of hydrogen sulfide thereby arresting the pyritization process and preservation of intermediate greigite mineral (Dewangan et al. 2013; Rowan and Roberts, 2006). Alternatively, the lack of sufficient amount of sulfur-oxidizers (Froelich et al. 1979) required to reduce sulfur (monosulfides) to stable iron sulfide (pyrite) can cause the disruption of pyritization processes leading to the formation of greigite. Silica diagenesis is an important process which occurs at methane-rich sites and could favour the formation of silicate-hosted magnetic mineral (oxides, sulfides) inclusions (Smrzka et al. 2015; Chang et al. 2016). Here, we report for the first time the occurrence of silicate-hosted iron sulfides (greigite) which is an important observation for understanding preservation of magnetic minerals in gas hydrate systems. We propose that paleo-methane seep created conducive environment for silica diagenesis and silicate weathering along with greigite formation. The re-precipitation of dissolved silica due to intense AOM might have embedded greigite as inclusions in silicate matrix.

#### **5. Conclusions**

The present study improves our understanding on the various constraints influencing the preservation of greigite in gas hydrate bearing sediments and its linkage with reactions involving methane. For the first time, we report the occurrence of diagenetically formed iron sulfides (greigite) nanoparticles as inclusions within silicate particles in greigite bearing sediment interval of core MD161/ Stn-8. This

is a new observation which is important for understanding the magnetic mineral diagenesis in gas hydrate settings.

FORC, TEM and SEM observations of magnetic particles from greigite bearing sediment helped in discriminating the complex magnetic mineral assemblages including detrital (titano-magnetite), diagenetic greigite occurring as nanoparticles inclusions within silicate particles and biogenic minerals. The results presented in this study should have wide applicability in unravelling the complex magnetic mineralogies in marine gas hydrate sedimentary system.

We propose that coupled silicate weathering and silica diagenesis triggered by paleo-methane seepage in K-G basin played an important role in preservation of greigite as inclusions in silicate matrix. Three scenarios explaining the potential constraints on the greigite preservation in marine sediments are presented. (Figs. 8a-c). Furthermore, we propose that the diagenetically formed greigite occurring as inclusions within silicate minerals can survive through geological times and thereby retain the magnetic characteristics crucial for palaeomagnetic studies.

### **Acknowledgements**

We thank the Directors of CSIR-NIO, NCAOR, NIOT, advisor MOES, and NGHP (India) for supporting this study. We thank head of oceanography department, and in-charge, on-board operations of IPEV are thanked for providing technical support and facilities onboard. We thank students of Goa University, IIT Kharagpur and the project scientists of NIO, NIOT, PRL and NGRI. We thank Dr. Mike Jackson, Institute for Rock Magnetism (IRM), University of Minnesota, USA for carrying out FORC measurements. We also thank the Director, Indian Institute of Geomagnetism (IIG), New Panvel, for providing permission to carry out magnetic measurements. We thank Professor B. R. Jagirdar, Indian Institute of Science, Bangalore, India for providing support with TEM-EDS analysis. We thank T. Ramprasad and Dr. Brenda Mascarenhas for suggestions and timely inputs in this work. This study was funded by SERB-DST, Government of India under the scheme “Early Career Research Award (DST no: ECR/2016/000528) to Dr. Firoz Badesab. The authors declare no conflicts of interests. We sincerely acknowledge the comments from the editor (Dr. Andrew Green), associate editor (Dr. Gerald Dickens) and two reviewers (Dr. Liao Chang and anonymous). The data used in this study can be made available upon email request to the corresponding author (firoz@nio.org). This is CSIR-NIO publication no. xxx.

## References

- Aloisi, G., Wallmann, K., Drews, M., & Bohrmann, G. (2004). Evidence for the submarine weathering of silicate minerals in Black Sea sediments: possible implications for the marine Li and B cycles. *Geochemistry, Geophysics, Geosystems*, 5(4). <https://doi.org/10.1029/2003GC000639>
- Badesab, F., Dewangan, P., Gaikwad, V., Kars, M., Kocherla, M., Krishna, K.S., Sangode, S.J., Deenadayalan, K., Kumar, P., Naikgaonkar, O., Ismaiel, M., and Khan, A. (2019). Magnetic mineralogical approach for exploration of gas hydrates in the Bay of Bengal. *Journal of Geophysical Research: Solid Earth*, 24 (5) pp. 4428-4451 <https://doi.org/10.1029/2019JB017466>.
- Badesab, F., Dewangan, P., Usapkar, A., Kocherla, M., Peketi, A., Mohite, K., Sangode, S.J. and Deenadayalan, K. (2017). Controls on evolution of gas-hydrate system in the Krishna-Godavari basin, offshore India. *Geochemistry, Geophysics, Geosystems*, 18(1), pp.52-74. <https://doi.org/10.1002/2016GC006606>
- Bazylinski, D. A., Frankel, R. B., Heywood, B. R., Mann, S., King, J. W., Donaghay, P. L., & Hanson, A. K. (1995). Controlled Biomineralization of Magnetite (Fe (inf3) O (inf4)) and Greigite (Fe (inf3) S (inf4)) in a Magnetotactic Bacterium. *Applied and Environmental Microbiology*, 61(9), 3232-3239.
- Berner, R. A. (1984). Sedimentary pyrite formation: an update. *Geochimica et Cosmochimica Acta*, 48(4), 605-615. [https://doi.org/10.1016/0016-7037\(84\)90089-9](https://doi.org/10.1016/0016-7037(84)90089-9)
- Biksham, G., and Subramanian, V. (1988). Sediment transport of the Godavari River basin and its controlling factors. *Journal of Hydrology*, 101(1-4), 275-290. [https://doi.org/10.1016/0022-1694\(88\)90040-6](https://doi.org/10.1016/0022-1694(88)90040-6)
- Canfield, D. E., & Raiswell, R. (1991). Taphonomy: releasing the data locked in the fossil record.
- Chang L, Roberts AP, Muxworthy AR, Tang Y, Chen Q, Rowan CJ, Liu Q, Pruner P. (2007). Magnetic characteristics of synthetic pseudo□single□domain and multi□domain greigite (Fe<sub>3</sub>S<sub>4</sub>). *Geophysical Research Letters*, 34(24). <https://doi.org/10.1029/2007GL032114>.
- Chang, L., Bolton, C.T., Dekkers, M.J., Hayashida, A., Heslop, D., Krijgsman, W., Kodama, K., Paterson, G.A., Roberts, A.P., Rohling, E.J., and Yamamoto, Y. (2016). Asian monsoon modulation of nonsteady state diagenesis in hemipelagic marine sediments offshore of Japan. *Geochemistry, Geophysics, Geosystems*, 17(11), pp.4383-4398. <https://doi.org/10.1002/2016GC006344>.
- Chang, L., Roberts, A.P., Heslop, D., Hayashida, A., Li, J., Zhao, X., Tian, W. and Huang, Q. (2016a). Widespread occurrence of silicate□hosted magnetic mineral inclusions in marine sediments and their contribution to paleomagnetic recording. *Journal of Geophysical Research: Solid Earth*, 121(12), pp.8415-8431. <https://doi.org/10.1002/2016JB013109>
- Chang, L., Heslop, D., Roberts, A. P., Rey, D., & Mohamed, K. J. (2016b). Discrimination of biogenic and detrital magnetite through a double Verwey transition temperature. *Journal of Geophysical Research: Solid Earth*, 121(1), 3-14. <https://doi.org/10.1002/2015JB012485>
- Chang, L., Roberts, A.P., Winklhofer, M., Heslop, D., Dekkers, M.J., Krijgsman, W., Fitz Gerald, J.D. and Smith, P. (2014a). Magnetic detection and characterization of biogenic magnetic minerals:

A comparison of ferromagnetic resonance and first-order reversal curve diagrams. *Journal of Geophysical Research: Solid Earth*, 119(8), pp.6136-6158. <https://doi.org/10.1002/2014JB011213>

Chang, L., Vasiliev, I., van Baak, C., Krijgsman, W., Dekkers, M.J., Roberts, A.P., Gerald, J.D.F., van Hoesel, A. and Winklhofer, M. (2014b). Identification and environmental interpretation of diagenetic and biogenic greigite in sediments: A lesson from the Messinian Black Sea. *Geochemistry, Geophysics, Geosystems*, 15(9), pp.3612-3627. <https://doi.org/10.1002/2014GC005411>

Chang, L., Winklhofer, M., Roberts, A.P., Dekkers, M.J., Horng, C.S., Hu, L. and Chen, Q., (2012). Ferromagnetic resonance characterization of greigite (Fe<sub>3</sub>S<sub>4</sub>), monoclinic pyrrhotite (Fe<sub>7</sub>S<sub>8</sub>), and non-interacting titanomagnetite (Fe<sub>3-x</sub>Ti<sub>x</sub>O<sub>4</sub>). *Geochemistry, Geophysics, Geosystems*, 13(5) <https://doi.org/10.1029/2012GC004063>.

Collett, T., Riedel, M., Cochran, J. R., Boswell, R., Presley, J., Kumar, P., Sathe, A., Lall, M., Sibal, V., and the NGHP Expedition 01 Scientists (2008). Indian National Gas Hydrate Program, Expedition - 01, Initial report, Directorate General of Hydrocarbons, Ministry of Petroleum and Natural Gas, India.

Cook, M. S., Keigwin, L. D., Birgel, D., and Hinrichs, K.-U., ( 2011), Repeated pulses of vertical methane flux recorded in glacial sediments from the southeast Bering Sea, *Paleoceanography*, 26, PA2210, doi:10.1029/2010PA001993.

Dewangan, P., Basavaiah N., Badesab F. K., Usapkar A., Mazumdar A., Joshi R., and Ramprasad T. (2013). Diagenesis of magnetic minerals in a gas hydrate/cold seep environment off the Krishna–Godavari basin, Bay of Bengal, *Marine Geology*, 340, 57–70, <https://doi.org/10.1016/j.margeo.2013.04.016>.

Dewangan, P., Sriram G., Ramprasad T., Ramana M. V., and Jaiswal P. (2011). Fault system and thermal regime in the vicinity of site NGHP-01-10, Krishna–Godavari basin, Bay of Bengal. *Marine and Petroleum Geology*, 28, 1899–1914, <https://doi.org/10.1016/j.marpetgeo.2011.03.009>.

Ebert, Y., Shaar, R., Emmanuel, S., Nowaczyk, N., and Stein, M. (2018). Overwriting of sedimentary magnetism by bacterially mediated mineral alteration. *Geology*, 46(4), 291-294. <https://doi.org/10.1130/G39706.1>

Egli, R., Chen, A. P., Winklhofer, M., Kodama, K. P., & Horng, C. S. (2010). Detection of noninteracting single domain particles using first-order reversal curve diagrams. *Geochemistry, Geophysics, Geosystems*, 11(1). <https://doi.org/10.1029/2009GC002916>.

Evans, M. E., & Wayman, M. L. (1970). An investigation of small magnetic particles by means of electron microscopy. *Earth and Planetary Science Letters*, 9(4), 365-370. [https://doi.org/10.1016/0012-821X\(70\)90137-8](https://doi.org/10.1016/0012-821X(70)90137-8)

Evans, M. E., McElhinny, M. W., & Gifford, A. C. (1968). Single domain magnetite and high coercivities in a gabbroic intrusion. *Earth and Planetary Science Letters*, 4(2), 142-146. [https://doi.org/10.1016/0012-821X\(68\)90008-3](https://doi.org/10.1016/0012-821X(68)90008-3)

Feinberg, J. M., R. J. Harrison, T. Kasama, R. E. Dunin-Borkowski, G. R. Scott, and P. R. Renne (2006). Effects of internal mineral structures on the magnetic remanence of silicate-hosted

titanomagnetite inclusions: An electron holography study. *Journal of Geophysical Research*, 111, B12S15, doi:10.1029/2006JB004498.

Feinberg, J. M., Scott, G. R., Renne, P. R., & Wenk, H. R. (2005). Exsolved magnetite inclusions in silicates: Features determining their remanence behavior. *Geology*, 33(6), 513-516. <https://doi.org/10.1130/G21290.1>

Froelich, P., Klinkhammer, G.P., Bender, M.L., Luedtke, N.A., Heath, G.R., Cullen, D., Dauphin, P., Hammond, D., Hartman, B., and Maynard, V. (1979). Early oxidation of organic matter in pelagic sediments of the eastern equatorial Atlantic: suboxic diagenesis. *Geochimica et Cosmochimica Acta*, 43(7), pp.1075-1090. [https://doi.org/10.1016/0016-7037\(79\)90095-4](https://doi.org/10.1016/0016-7037(79)90095-4)

Harrison, R. J., & Feinberg, J. M. (2008). FORCinel: An improved algorithm for calculating first-order reversal curve distributions using locally weighted regression smoothing. *Geochemistry, Geophysics, Geosystems*, 9, Q05016. <https://doi.org/10.1029/2008GC001987>.

Horng, C. S., and Chen, K. H. (2006). Complicated magnetic mineral assemblages in marine sediments offshore southwestern Taiwan: Possible influences of methane flux on the early diagenetic process. *Terrestrial, Atmospheric and Oceanic Sciences*, 17, 1009–1026. [https://doi.org/10.3319/TAO.2006.17.4.1009\(GH\)](https://doi.org/10.3319/TAO.2006.17.4.1009(GH))

Hounslow, M. W., & Morton, A. C. (2004). Evaluation of sediment provenance using magnetic mineral inclusions in clastic silicates: comparison with heavy mineral analysis. *Sedimentary Geology*, 171(1-4), 13-36. <https://doi.org/10.1016/j.sedgeo.2004.05.008>

Housen, B. A., and Musgrave, R. J. (1996). Rock-magnetic signature of gas hydrates in accretionary prism sediments. *Earth and Planetary Science Letters*, 139(3-4), 509-519. [https://doi.org/10.1016/0012-821X\(95\)00245-8](https://doi.org/10.1016/0012-821X(95)00245-8)

Jørgensen, B. B., Böttcher, M. E., Lüschen, H., Neretin, L. N., & Volkov, I. I. (2004). Anaerobic methane oxidation and a deep H<sub>2</sub>S sink generate isotopically heavy sulfides in Black Sea sediments. *Geochimica et Cosmochimica Acta*, 68(9), 2095-2118. <https://doi.org/10.1016/j.gca.2003.07.017>

Joshi, R.K., Mazumdar, A., Peketi, A., Ramamurty, P.B., Naik, B.G., Kocherla, M., Carvalho, M.A., Mahalakshmi, P., Dewangan, P. and Ramana, M.V. (2014). Gas hydrate destabilization and methane release events in the Krishna–Godavari Basin, Bay of Bengal. *Marine and Petroleum Geology*, 58, pp.476-489. <https://doi.org/10.1016/j.marpetgeo.2014.08.013>

Kao, S. J., Horng, C. S., Roberts, A. P., & Liu, K. K. (2004). Carbon–sulfur–iron relationships in sedimentary rocks from southwestern Taiwan: influence of geochemical environment on greigite and pyrrhotite formation. *Chemical Geology*, 203(1-2), 153-168. <https://doi.org/10.1016/j.chemgeo.2003.09.007>

Kars, M. M., and Kodma K. (2015a), Authigenesis of magnetic minerals in gas hydrate bearing sediments in the Nankai Trough, Offshore Japan, *Geochemistry, Geophysics, Geosystems*, 16, 947–961, <https://doi.org/10.1002/2014GC005614>.

Kasten, S., Freudenthal T., Gingele F. X., and Schulz H. D. (1998), Simultaneous formation of iron-rich layers at different redox boundaries in sediments of the Amazon deep-sea fan, *Geochimica et Cosmochimica Acta*, 62, 2253–2264, [https://doi.org/10.1016/S0016-7037\(98\)00093-3](https://doi.org/10.1016/S0016-7037(98)00093-3).

- Kiel, S., Birgel, D., Campbell, K.A., Crampton, J.S., Schiøler, P., Peckmann, J., 2013. Cretaceous methane-seep deposits from New Zealand and their fauna. *Palaeogeogr.Palaeoclimatol. Palaeoecol.* 390, 17–34, doi: <https://doi.org/10.1016/j.palaeo.2012.10.033>
- Kim, J. H., Torres, M. E., Haley, B. A., Ryu, J. S., Park, M. H., Hong, W. L., & Choi, J. (2016). Marine silicate weathering in the anoxic sediment of the Ulleung Basin: Evidence and consequences. *Geochemistry, Geophysics, Geosystems*, 17(8), 3437-3453. <https://doi.org/10.1002/2016GC006356>
- Kumar, P., Collett, T.S., Boswell, R., Cochran, J.R., Lall, M., Mazumdar, A., Ramana, M.V., Ramprasad, T., Riedel, M., Sain, K., and Sathe, A.V. (2014). Geologic implications of gas hydrates in the offshore of India: Krishna-Godavari Basin, Mahanadi Basin, Andaman Sea, Kerala–Konkan Basin. *Marine and Petroleum Geology*, 58, pp.29-98. <https://doi.org/10.1016/j.marpetgeo.2014.07.031>
- Kuechler, R.R., Birgel, D., Kiel, S., Freiwald, A., Goedert, J.L., Thiel, V., Peckmann, J., (2012). Miocene methane-derived carbonates from southwestern Washington, USA and a model for silicification at seeps. *Lethaia* 45, 259–273, doi: <https://doi.org/10.1111/j.1502-3931.2011.00280.x>
- Larrasoña, J. C., Murelaga, X., & Garcés, M. (2006). Magnetobiochronology of Lower Miocene (Ramblian) continental sediments from the Tudela formation (western Ebro basin, Spain). *Earth and Planetary Science Letters*, 243(3-4), 409-423. <https://doi.org/10.1016/j.epsl.2006.01.034>
- Larrasoana, J. C., Roberts, A. P., Chang, L., Schellenberg, S. A., Gerald, J. D. F., Norris, R. D., & Zachos, J. C. (2012). Magnetotactic bacterial response to Antarctic dust supply during the Palaeocene–Eocene thermal maximum. *Earth and Planetary Science Letters*, 333, 122-133. <https://doi.org/10.1016/j.epsl.2012.04.003>
- Larrasoña, J. C., Roberts, A. P., Musgrave, R. J., Gràcia, E., Piñero, E., Vega, M., and Martínez-Ruiz, F. (2007). Diagenetic formation of greigite and pyrrhotite in gas hydrate marine sedimentary systems. *Earth and Planetary Science Letters*, 261(3-4), 350-366. <https://doi.org/10.1016/j.epsl.2007.06.032>
- Lascu, I., Einsle, J. F., Ball, M. R., and Harrison, R. J. (2018). The vortex state in geologic materials: A micromagnetic perspective. *Journal of Geophysical Research: Solid Earth*, 123, 7285–7304. <https://doi.org/10.1029/2018JB015909>
- Lee, M. W., & Collett, T. S. (2009). Gas hydrate saturations estimated from fractured reservoir at Site NGHP-01-10, Krishna–Godavari Basin, India. *Journal of Geophysical Research: Solid Earth*, 114(B7). <https://doi.org/10.1029/2008JB006237>
- Maher, B. A. (1988). Magnetic properties of some synthetic sub-micron magnetites. *Geophysical Journal International*, 94(1), 83-96. <https://doi.org/10.1111/j.1365-246X.1988.tb03429.x>
- Mazumdar, A., Dewangan, P., João, H.M., Peketi, A., Khosla, V.R., Kocherla, M., Badesab, F.K., Joshi, R.K., Roxanne, P., Ramamurty, P.B., & Karisiddaiah, S.M., (2009). Evidence of paleo–cold seep activity from the Bay of Bengal, offshore India. *Geochemistry, Geophysics, Geosystems*, 10(6). <https://doi.org/10.1029/2008GC002337>.



- Mazumdar, A., Joshi, R. K., Peketi, A., and Kocherla, M., (2011), Occurrence of faecal pellet-filled simple and composite burrows in cold seep carbonates: A glimpse of a complex benthic ecosystem. *Marine. Geology*, 289, 117–121, doi:10.1016/j.margeo.2011.09.003.
- Mazumdar, A., Dewangan, P., Peketi, A., Sriram, G., Kalpana, M.S., Naik, G.P., Shetty, D., Pujari, S., Pillutla, S.P., Gaikwad, V.V., Nazareth, D., Sangodkar, N.S., Dakara, G., Kumar, A., Mishra, C.K., Singha, P., Reddy, R., (2019), The first record of active methane (cold) seep ecosystem from the Indian EEZ, 128:18, *Journal of Earth System Science*, doi: 10.1007/s12040-018-1044-y.
- Morgan, G. E., & Smith, P. P. K. (1981). Transmission electron microscope and rock magnetic investigations of remanence carriers in a Precambrian metadolerite. *Earth and Planetary Science Letters*, 53(2), 226-240. [https://doi.org/10.1016/0012-821X\(81\)90156-4](https://doi.org/10.1016/0012-821X(81)90156-4)
- Musgrave, R. J., Bangs, N. L., Larrasoana, J. C., Gràcia, E., Hollamby, J. A., and Vega, M. E. (2006). Rise of the base of the gas hydrate zone since the last glacial recorded by rock magnetism. *Geology*, 34(2), 117-120. <https://doi.org/10.1130/G22008.1>
- Muxworthy, A. R., and Dunlop, D. J. (2002). First-order reversal curve (FORC) diagrams for pseudo-single-domain magnetites at high temperature. *Earth and Planetary Science Letters*, 203(1), 369-382. [https://doi.org/10.1016/S0012-821X\(02\)00880-4](https://doi.org/10.1016/S0012-821X(02)00880-4)
- Muxworthy, A. R., Williams, W., Roberts, A. P., Winklhofer, M., Chang, L., & Posfai, M. (2013). Critical single domain grain sizes in chains of interacting greigite particles: Implications for magnetosome crystals. *Geochemistry, Geophysics, Geosystems*, 14(12), 5430-5441. <https://doi.org/10.1002/2013GC004973>
- Oldfield, F. (2007). Sources of fine-grained magnetic minerals in sediments: a problem revisited. *The Holocene*, 17(8), 1265-1271. <https://doi.org/10.1177/0959683607085135>
- Peketi, A., Mazumdar, A., Joshi, R. K., Patil, D. J., Srinivas, P. L., and Dayal, A. M. (2012), Tracing the paleo sulfate–methane transition zones and H<sub>2</sub>S seepage events in marine sediments: An application of C-S-Mo systematic. *Geochemistry, Geophysics, Geosystems*, 13, Q10007, <https://doi.org/10.1029/2012GC004288>.
- Petersen, N., T. Von Dobeneck, and H. Vali (1986), Fossil bacterial magnetite in deep-sea sediments from the South Atlantic Ocean, *Nature*, 320, 611–615, <https://doi.org/10.1038/320611a0>.
- Pike, C. R., Roberts, A. P., and Verosub, K. L. (1999). Characterizing interactions in fine magnetic particle systems using first order reversal curves. *Journal of Applied Physics*, 85(9), 6660-6667. <https://doi.org/10.1063/1.370176>
- Prabhakar, K. N., and Zutshi, P.L. (1993). Evolution of southern part of Indian East Coast basin. *Journal of Geological Society of India*, 41, 215-230.
- Ramesh R., and V. Subramanian (1988), Temporal, spatial and size variation in the sediment transport in the Krishna River basin, India, *Journal of Hydrology*, 98, 53–65. [https://doi.org/10.1016/0022-1694\(88\)90205-3](https://doi.org/10.1016/0022-1694(88)90205-3)
- Rao, G. N. (2001). Sedimentation, stratigraphy, and petroleum potential of Krishna-Godavari basin, East Coast of India. *American Association of Petroleum Geologists bulletin*, 85(9), 1623-1643.

- Reinholdsson, M., Snowball, I., Zillén, L., Lenz, C., & Conley, D. J. (2013). Magnetic enhancement of Baltic Sea sapropels by greigite magnetofossils. *Earth and Planetary Science Letters*, 366, 137-150. <https://doi.org/10.1016/j.epsl.2013.01.029>
- Roberts, A. P. (2015). Magnetic mineral diagenesis. *Earth-Science Reviews*, 151, 1-47. <https://doi.org/10.1016/j.earscirev.2015.09.010>
- Roberts, A. P., and Turner, G. M. (1993). Diagenetic formation of ferrimagnetic iron sulphide minerals in rapidly deposited marine sediments, South Island, New Zealand. *Earth and Planetary Science Letters*, 115(1-4), 257-273. [https://doi.org/10.1016/0012-821X\(93\)90226-Y](https://doi.org/10.1016/0012-821X(93)90226-Y)
- Roberts, A. P., Chang, L., Rowan, C. J., Horng, C. S., & Florindo, F. (2011b). Magnetic properties of sedimentary greigite (Fe<sub>3</sub>S<sub>4</sub>): An update. *Reviews of Geophysics*, 49, RG1002. <https://doi.org/10.1029/2010RG000336>
- Roberts, A. P., Chang, L., Rowan, C. J., Horng, C. S., & Florindo, F. (2011a). Magnetic properties of sedimentary greigite (Fe<sub>3</sub>S<sub>4</sub>): An update. *Reviews of Geophysics*, 49(1).
- Roberts, A. P., Liu, Q., Rowan, C. J., Chang, L., Carvallo, C., Torrent, J., & Horng, C. S. (2006). Characterization of hematite ( $\alpha$ -Fe<sub>2</sub>O<sub>3</sub>), goethite ( $\alpha$ -FeOOH), greigite (Fe<sub>3</sub>S<sub>4</sub>), and pyrrhotite (Fe<sub>7</sub>S<sub>8</sub>) using first-order reversal curve diagrams. *Journal of Geophysical Research: Solid Earth*, 111(B12). <https://doi.org/10.1029/2006JB004715>
- Roberts, A. P., Pike, C. R., and Verosub, K. L. (2000). First-order reversal curve diagrams: A new tool for characterizing the magnetic properties of natural samples. *Journal of Geophysical Research: Solid Earth*, 105(B12), 28461-28475. <https://doi.org/10.1029/2000JB900326>
- Roberts, A. P., Stoner, J. S., & Richter, C. (1999). Diagenetic magnetic enhancement of sapropels from the eastern Mediterranean Sea. *Marine Geology*, 153(1-4), 103-116. [https://doi.org/10.1016/S0025-3227\(98\)00087-5](https://doi.org/10.1016/S0025-3227(98)00087-5)
- Roberts, A.P., Almeida, T.P., Church, N.S., Harrison, R.J., Heslop, D., Li, Y., Li, J., Muxworthy, A.R., Williams, W. and Zhao, X. (2017). Resolving the origin of pseudo-single domain magnetic behavior. *Journal of Geophysical Research: Solid Earth*, 122(12), pp.9534-9558. <https://doi.org/10.1002/2017JB014860>
- Rowan, C. J., and Roberts, A. P. (2006). Magnetite dissolution, diachronous greigite formation, and secondary magnetizations from pyrite oxidation: Unravelling complex magnetizations in Neogene marine sediments from New Zealand. *Earth and Planetary Science Letters*, 241(1-2), 119-137. <https://doi.org/10.1016/j.epsl.2005.10.017>
- Scholz, F., Hensen, C., Schmidt, M., & Geersen, J. (2013). Submarine weathering of silicate minerals and the extent of pore water freshening at active continental margins. *Geochimica et Cosmochimica Acta*, 100, 200-216. <https://doi.org/10.1016/j.gca.2012.09.043>
- Smrzka, D., Kraemer, S.M., Zwicker, J., Birgel, D., Fischer, D., Kasten, S., Goedert, J.L., & Peckmann, J., (2015). Constraining silica diagenesis in methane-seep deposits. *Palaeogeography, Palaeoclimatology, Palaeoecology*, 420, pp.13-26.

Snowball, I. F. (1994). Bacterial magnetite and the magnetic properties of sediments in a Swedish lake. *Earth and Planetary Science Letters*, 126(1-3), 129-142. [https://doi.org/10.1016/0012-821X\(94\)90246-1](https://doi.org/10.1016/0012-821X(94)90246-1)

Snowball, I. F. (1997a). Gyroremanent magnetization and the magnetic properties of greigite-bearing clays in southern Sweden. *Geophysical Journal International*, 129(3), 624-636. <https://doi.org/10.1111/j.1365-246X.1997.tb04498.x>

Snowball, I., Sandgren, P., & Petterson, G. (1999). The mineral magnetic properties of an annually laminated Holocene lake-sediment sequence in northern Sweden. *The Holocene*, 9(3), 353-362. <https://doi.org/10.1191/095968399670520633>

Snowball, I., Zillén, L., & Sandgren, P. (2002). Bacterial magnetite in Swedish varved lake-sediments: a potential bio-marker of environmental change. *Quaternary International*, 88(1), 13-19. [https://doi.org/10.1016/S1040-6182\(01\)00069-6](https://doi.org/10.1016/S1040-6182(01)00069-6)

Solomon, E. A., Spivack, A. J., Kastner, M., Torres, M. E., & Robertson, G. (2014). Gas hydrate distribution and carbon sequestration through coupled microbial methanogenesis and silicate weathering in the Krishna–Godavari Basin, offshore India. *Marine and Petroleum Geology*, 58, 233-253. <https://doi.org/10.1016/j.marpetgeo.2014.08.020>

Sriram, G., Dewangan, P., Ramprasad, T., & Rama Rao, P. (2013). Anisotropic amplitude variation of the bottom-simulating reflector beneath fracture-filled gas hydrate deposit. *Journal of Geophysical Research: Solid Earth*, 118(5), 2258-2274. <https://doi.org/10.1002/jgrb.50176>

Stolz, J. F., Chang, S. B. R., & Kirschvink, J. L. (1986). Magnetotactic bacteria and single-domain magnetite in hemipelagic sediments. *Nature*, 321(6073), 849. <https://doi.org/10.1038/321849a0>

Vasiliev, I., Dekkers, M. J., Krijgsman, W., Franke, C., Langereis, C. G., & Mullender, T. A. (2007). Early diagenetic greigite as a recorder of the palaeomagnetic signal in Miocene–Pliocene sedimentary rocks of the Carpathian foredeep (Romania). *Geophysical Journal International*, 171(2), 613-629. <https://doi.org/10.1111/j.1365-246X.2007.03560.x>

Vasiliev, I., Franke, C., Meeldijk, J. D., Dekkers, M. J., Langereis, C. G., & Krijgsman, W. (2008). Putative greigite magnetofossils from the Pliocene epoch. *Nature Geoscience*, 1(11), 782. <https://doi.org/10.1038/ngeo335>

Wakabayashi, K., H. Tsunakawa, N. Mochizuki, Y. Yamamoto, and Y. Takigami (2006), Paleomagnetism of the Middle Cretaceous Iritono granite in the Abukuma region, northeast Japan, *Tectonophysics*, 421, 161–171. <https://doi.org/10.1016/j.tecto.2006.04.013>

Wallmann, K., Aloisi, G., Haeckel, M., Tishchenko, P., Pavlova, G., Greinert, J., Kutterolf, S. and Eisenhauer, A. (2008). Silicate weathering in anoxic marine sediments. *Geochimica et Cosmochimica Acta*, 72(12), pp.2895-2918. <https://doi.org/10.1016/j.gca.2008.03.026>

Wallmann, K., Riedel, M., Hong, W.L., Patton, H., Hubbard, A., Pape, T., Hsu, C.W., Schmidt, C., Johnson, J.E., Torres, M.E. and Andreassen, K. (2018). Gas hydrate dissociation off Svalbard induced by isostatic rebound rather than global warming. *Nature communications*, 9(1), p.83. <https://doi.org/10.1038/s41467-017-02550-9>

Yamazaki, T. (2012). Paleoposition of the Intertropical Convergence Zone in the eastern Pacific inferred from glacial-interglacial changes in terrigenous and biogenic magnetic mineral fractions. *Geology*, 40(2), 151-154. <https://doi.org/10.1130/G32646.1>

### Figure captions:

**Figure 1.** Map showing the location of sediment cores MD161/Stn-8 and NGHP-01-10D off Krishna-Godavari (K-G) basin, Bay of Bengal.

**Figure 2.** Down-core profiles of environmental magnetic parameters (a) Magnetic susceptibility ( $\chi$ ), (b) frequency-dependent magnetic susceptibility  $\chi_{fd}$ (%); Geochemical parameters (c) CRS (wt %), (d) Mo(ppm) and (e)  $\delta^{34}\text{S}_{\text{CRS}}$  (VCDT ‰); FORC diagrams (e) 20.72 mbsf (diagenetic greigite) (f) 22.70 mbsf (biogenic greigite) for sediment core MD161/Stn-8. The zone of increased magnetic susceptibility (greigite) from 17.0 mbsf - 23.0 m is highlighted by a blue band.

**Figure 3.** Comparison of FORC distributions for selected samples from greigite zone of core MD161/Stn-8. (a) 20.98 mbsf, (b) 22.38 mbsf, and (c) 22.44 mbsf. FORC distributions for samples from 20.98 mbsf, 22.38 mbsf are characterized by a peak at  $B_C \sim 10$  mT with closed contours indicating vortex-state behavior of magnetic particles behaviour (Lascu et al. 2018; Muxworthy & Dunlop 2002; Roberts et al. 2000; Roberts et al. 2017) (**Figs. 3a, 3b**). The FORC diagram for sample from 22.44 mbsf (Fig. 3c) showed a central ridge signature with a peak fields changing between  $\sim 10$  and 40 mT suggesting the presence of biogenic magnetite (Chang et al., 2014b).

**Figure 4.** Scanning electron microscope images (secondary electron) on magnetic extracts from sediment core MD161/Stn-8. (a) & (d) magnetites (20.84 mbsf and 22.88 mbsf) and (b), c, (e), (f) pyrite (17.42 mbsf, 19.4 mbsf, 23.54 mbsf, 23.62 mbsf). Please note that pyrite is marked as (P) and magnetite with (M).

**Figure 5.** Photographs of magnetic grains extracted from greigite zone of core MD161/Stn-8. The grains were observed with optical microscope under reflected light. The magnetic grains extracted from greigite zone (sample 22.66 mbsf) of core MD161/Stn-8 showed pyrite (orange-reddish color) overgrowths probably on magnetite grain

**Figure 6.** TEM images of magnetic extracts from greigite zone in core MD161/Stn-8. (a) 20.72 mbsf, (b) 21.52 mbsf (c) 22.52 mbsf (d) 22.70 mbsf, (e) 22.34 mbsf, and (f) 22.64 mbsf. Please note that greigite is marked as (G) and magnetite with (M).

**Figure 7.** Down-core profiles of (a) magnetic susceptibility ( $\chi_{lf}$ ) and pore-water (b) dissolved silica, and (c) alkalinity concentrations at NGHP-01-10D (close to drilled site Site MD161/Stn-8).

**Figure 8.** Conceptual model explaining the controls on greigite preservation at site MD161/Stn-8 / in K-G basin.

**Supplementary Figure S1:** Down-core variations in (a) magnetic susceptibility ( $\chi_{lf}$ ), (b) SIRM/ $\chi$ , (c)  $\chi_{fd}$ % and (d) total organic carbon (TOC) at site MD161/Stn-8.

**Supplementary Figure S2:** Correlation of magnetic susceptibility between two sediment cores (MD161/Stn-8, NGHP-01-10D) from Krishna-Godavari basin.

**Figure. 1**

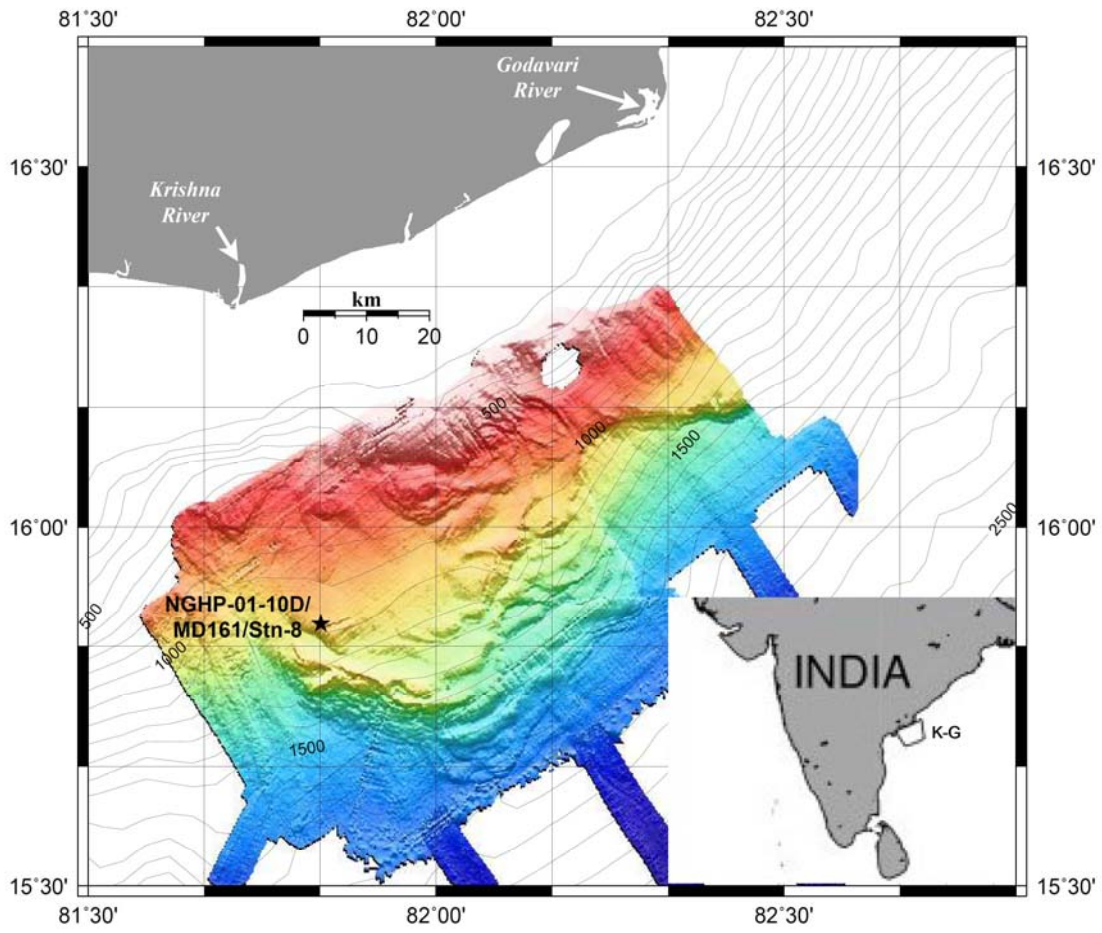


Figure. 2

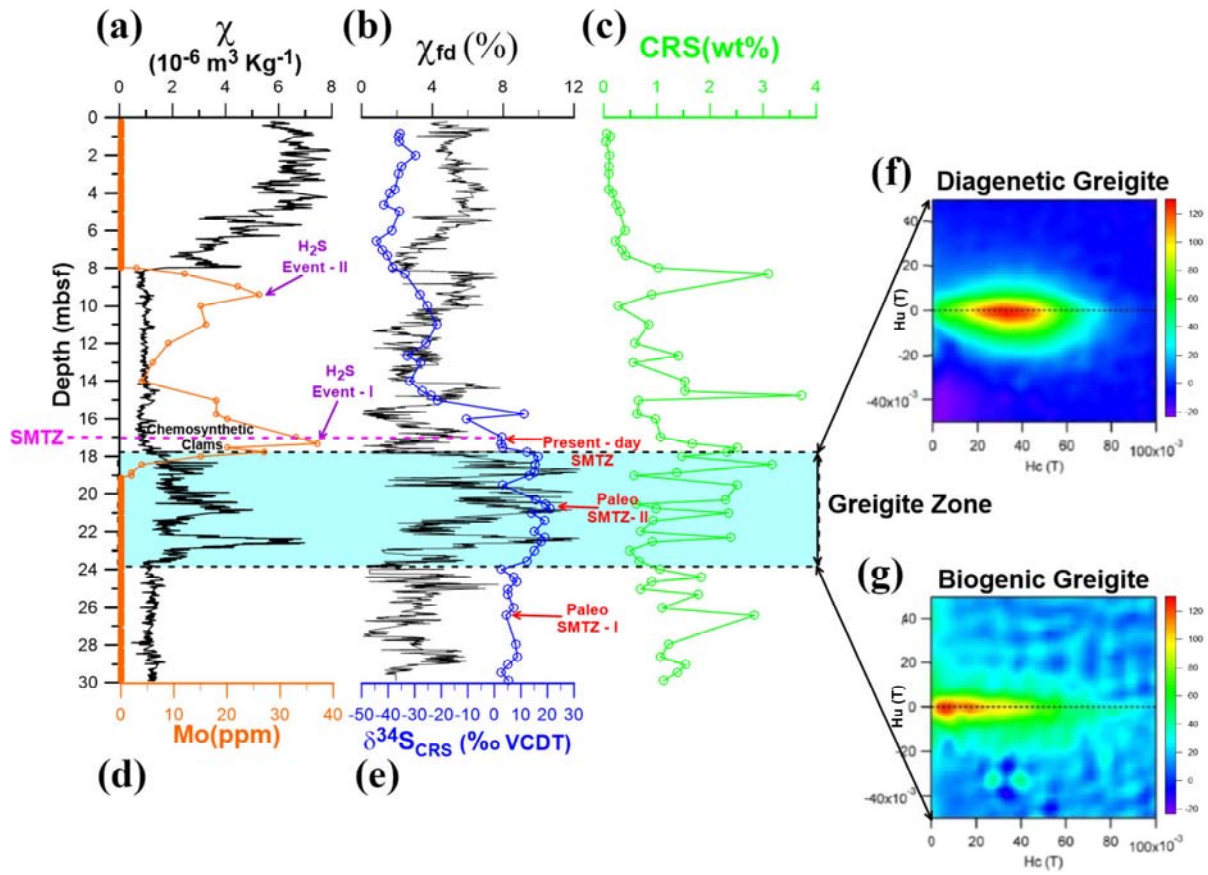


Figure. 3

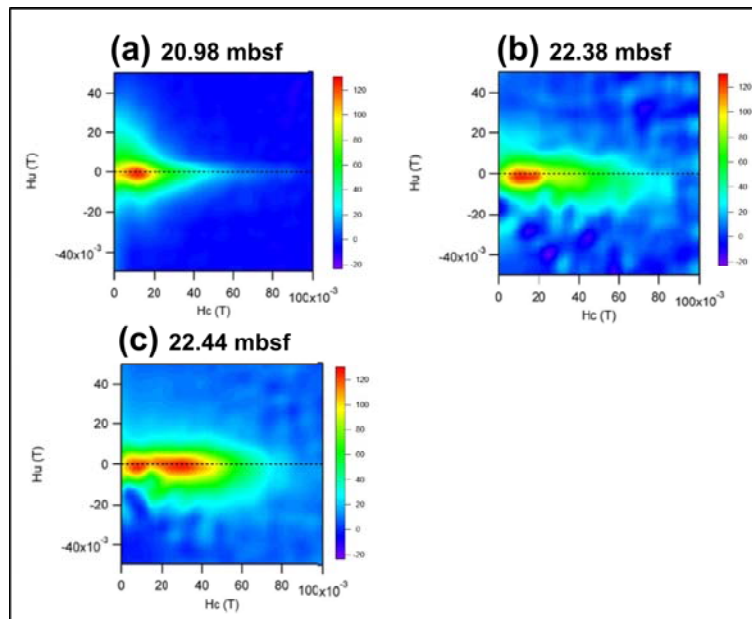


Figure. 4

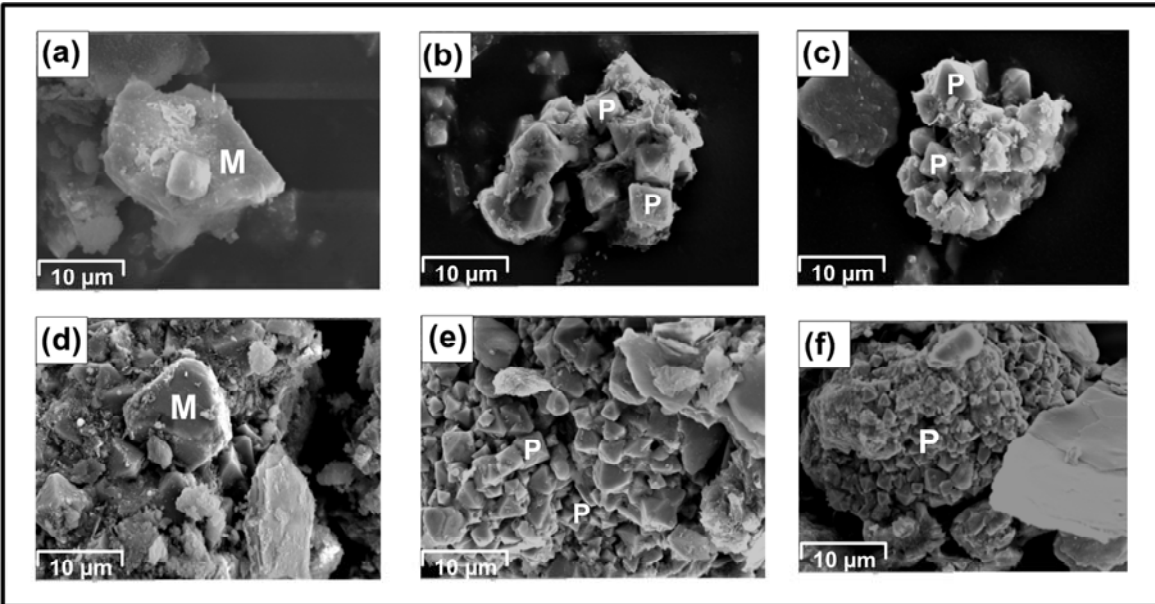


Figure. 5

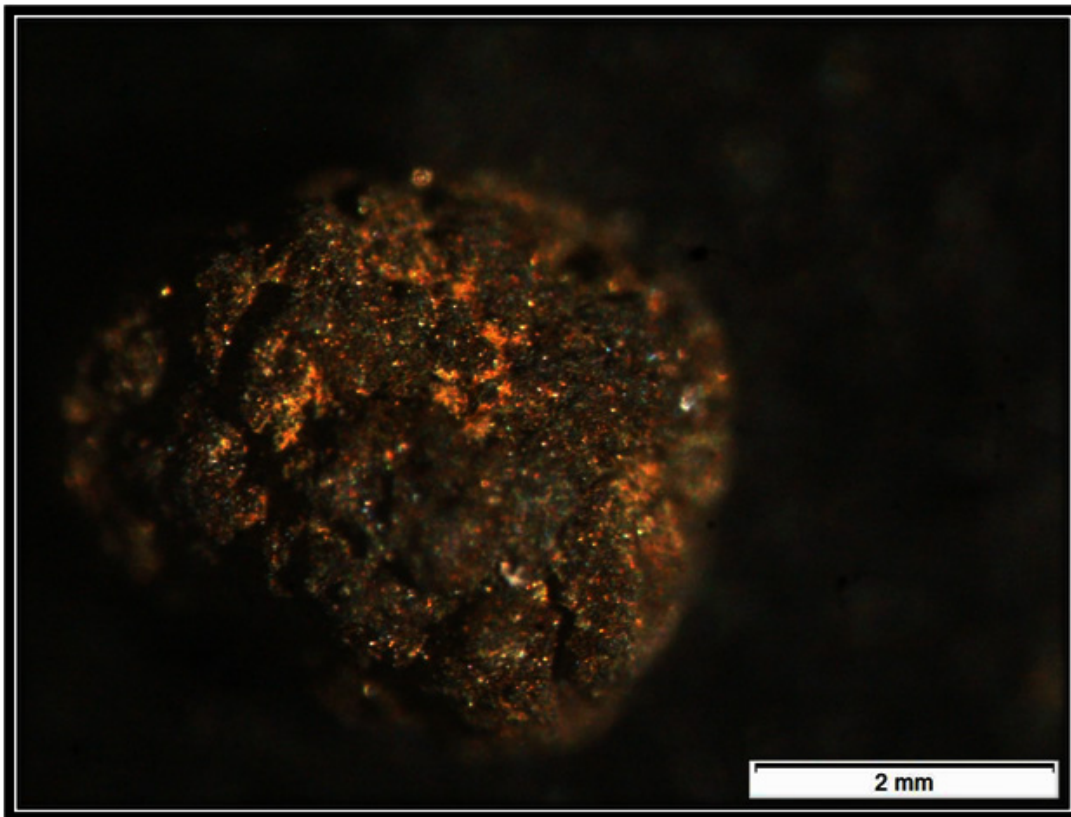


Figure. 6

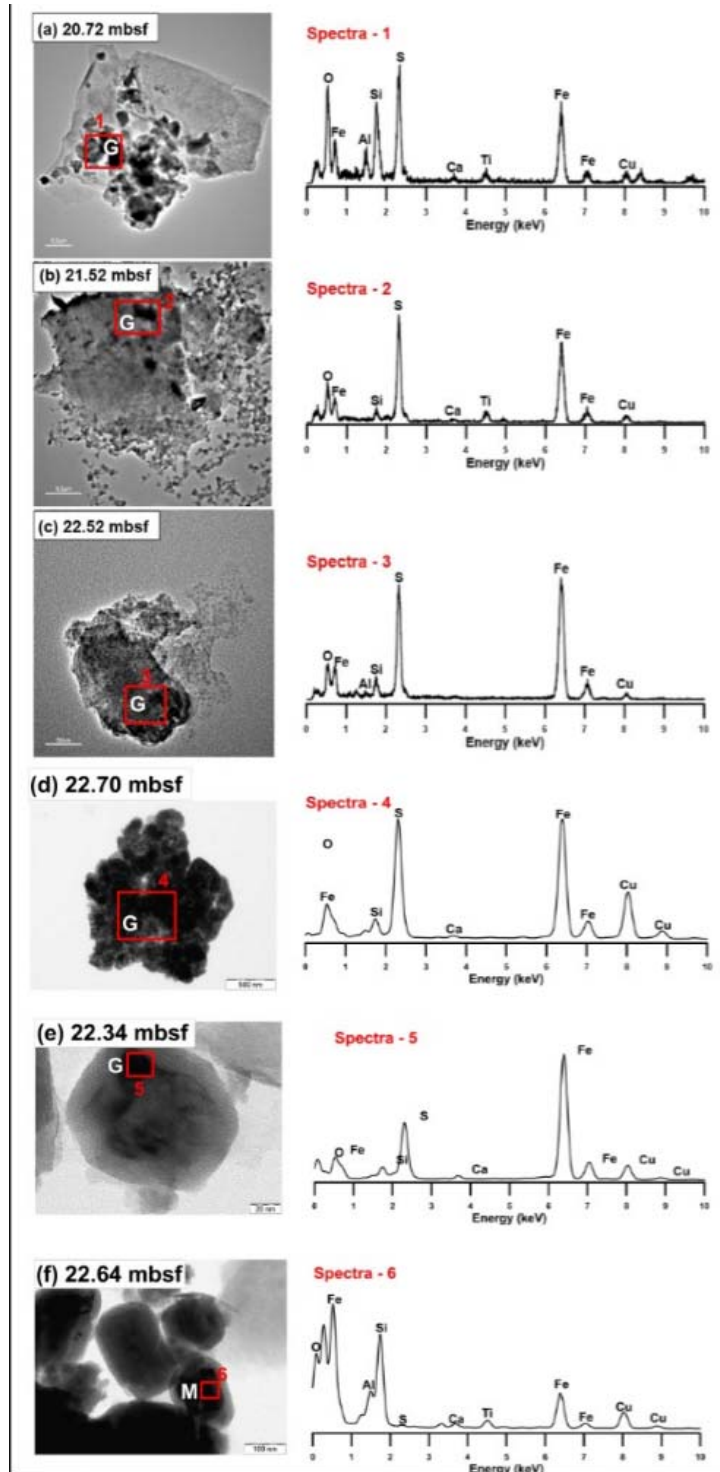




Figure. 7

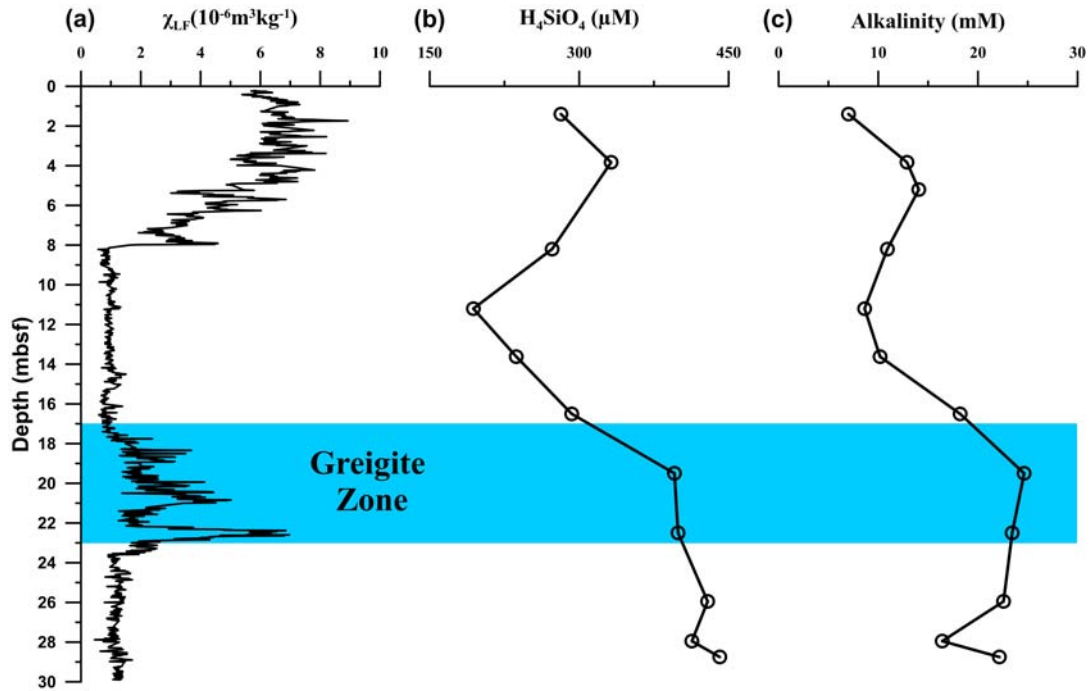
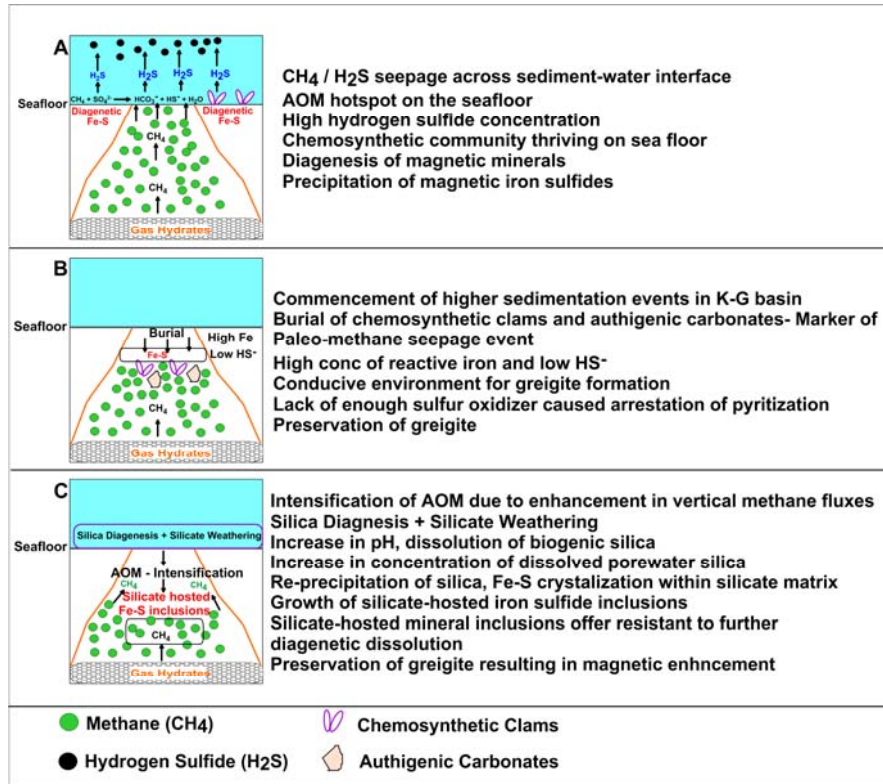
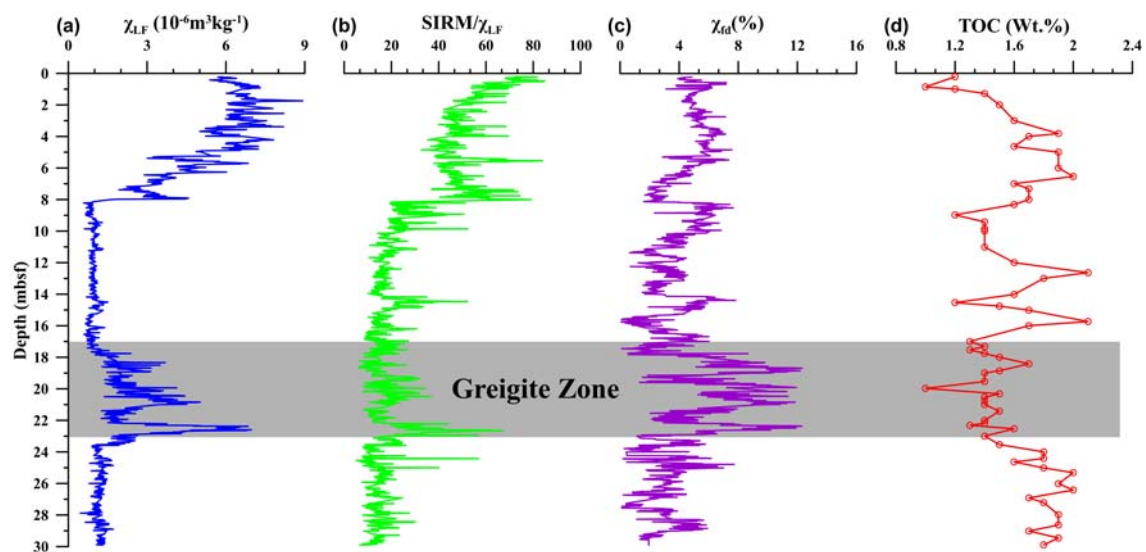


Figure. 8



Supplementary Fig. S1



Supplementary Fig. S2

